

Turbo Estimation and Equalization for Asynchronous Uplink MC-CDMA

M. Guenach, *Member, IEEE*, M. Marey, H. Wymeersch, *Member, IEEE*, H. Steendam, *Senior Member, IEEE*, and M. Moeneclaey, *Fellow, IEEE*

Abstract—In this contribution, we propose a new code-aided synchronization and channel estimation algorithm for uplink MC-CDMA. The space alternating generalized expectation-maximization (SAGE) algorithm is used to estimate the channel impulse responses, propagation delays and carrier frequency offsets of the different users. The estimator, multi-user detector, equalizer, demapper and channel decoder exchange soft information in an iterative way. The performance of the proposed algorithm is evaluated through Monte Carlo simulations. Impressive performance gains are visible as compared to a conventional data-aided estimation scheme.

Index Terms—Synchronization, estimation, code-aided, turbo equalization, asynchronous MC-CDMA, uplink.

I. INTRODUCTION

ORTHOGONAL frequency division multiplexing (OFDM) is one of the most promising modulation schemes for current and next-generation wireless and wireline communications [1], [2]. Its capability to accommodate high data rate transmissions over frequency selective channels while allowing for a simple equalization makes it a very attractive technology. However, OFDM-based transmission systems are very sensitive to synchronization errors [3], [4]. Accurate timing and frequency synchronization is required to maintain orthogonality among subcarriers and to avoid inter-symbol-interference (ISI). Additionally, the channel impulse response (CIR) must be known to coherently detect the data. When we consider the massive amount of research devoted to these problems (see e.g. [4]–[13] and references therein), it becomes clear that synchronization and channel estimation are critical issues. The conventional estimation techniques are either *data-aided* (DA) (i.e., exploiting training symbols in the time- or frequency domain) [5]–[10] or *blind* (e.g., exploiting the presence of the cyclic prefix) [11]–[13].

Manuscript received August 30, 2006; revised December 19, 2006 and February 24, 2007; accepted March 20, 2007. The associate editor coordinating the review of this paper and approving it for publication was G. Vitetta. M. Marey thanks the Egyptian government for its financial support. H. Wymeersch gratefully acknowledges the support of the Belgian American Educational Foundation.

M. Guenach is with Alcatel-Lucent Bell Labs Antwerp (e-mail: guenach@ieee.org).

M. Marey, H. Steendam, and M. Moeneclaey are with the TELIN Department, Ghent University, St.-Pietersnieuwstraat 41, B-9000 GENT, Belgium (e-mail: {mohamed, hs, mm}@telin.UGent.be).

H. Wymeersch is with the Laboratory for Information and Decision Systems, Massachusetts Institute of technology, Cambridge, MA (e-mail: hwymeersch@mit.edu).

Digital Object Identifier 10.1109/TWC.2008.060648.

With the advent of powerful error-correcting codes, these conventional techniques cannot always be applied successfully. Powerful codes lead to a combination of low BER at low SNR, a challenging operating point to perform estimation. At these low SNRs, blind techniques are completely unreliable. On the other hand, data-aided algorithms require an unreasonable amount of power and bandwidth to be reserved for training. This has spurred several research groups to consider *code-aided* or *code-aware* estimation algorithms. These algorithms iterate between data detection and estimation, thus improving both the estimates of synchronization parameters and impulse responses, while simultaneously performing increasingly reliable data detection. Such techniques are often inspired by the turbo-principle [14] or the Expectation-Maximization (EM) algorithm [15], [16]. In [17], an EM-based semi-blind technique is described which performs code-aided estimation of the CIR per Multi-Carrier (MC) symbol. The same idea was applied in the frequency domain in [18] for a multi-antenna, multi-user system. The EM algorithm was again considered in [19] for estimation of the CIR for a time-varying MIMO-OFDM scenario. Finally, [20] proposes an ad-hoc code-aided channel estimator for time-varying OFDM systems.

The current contribution is focused on timing, carrier frequency offset (CFO) and CIR estimation for uplink MC-CDMA. Existing uplink multiuser MC synchronization methods can be categorized into two classes. The first class considers a scenario where it is assumed that only one new user's frequency and time offsets need to be estimated while other users have already been perfectly synchronized to the base station [5], [21]. Hence, this approach estimates frequency and timing offsets for only one user and does not fully represent a practical situation. The second category addresses multiple unsynchronized users scenarios such as [22]–[24]. In [22], a low complexity maximum likelihood (ML) DA synchronization and channel estimation scheme is investigated in the uplink of quasi-synchronous OFDMA system by means of alternating-projection, while [23] applies the SAGE to perform joint frequency synchronization, channel estimation and data detection. Finally [24] considers channel tracking by means of least mean squares approach, and reports negligible performance loss for mobile speeds up to 90km/h.

All these papers on MC-CDMA have in common that they do not exploit any properties of the underlying error-correcting code. It is therefore necessary to investigate code-aided algorithms for MC-CDMA. In our companion paper [25] we derived a code-aided algorithm for *downlink* MC-CDMA

TABLE I
NOTATIONS

notation	meaning
i	MC symbol index: $0 \leq i < M$
k	user index: $1 \leq k \leq K_u$
s	chip index: $0 \leq s < N_s$
m	time-domain index: $-\nu \leq m < N = N_s P$
p	data symbol index: $0 \leq p < P$
ξ	SAGE iteration index: $0 \leq \xi$

channel estimation and synchronization. The *uplink* scenario, which is the topic of this paper, is much more challenging than the downlink scenario. Since the base station must recover the signal from all users, we are now dealing with a multiuser detection problem, as opposed to single-user detection in the downlink. From an estimation/synchronization point of view, this implies that more sophisticated algorithms must be applied (as we will see, SAGE instead of EM). A major challenge, as compared to [25], is coping with the different delays and CFOs of the different users. As relative delays may exceed the duration of the cyclic prefix, a combination of time-domain and frequency-domain techniques are required to successfully recover the data of all the users. Starting from the maximum a posteriori (MAP) principle, we derive an estimation algorithm based on the SAGE algorithm, exploiting information from the pilot symbols and coded data symbols in a systematic fashion. It is noteworthy that the designed estimation scheme can work with any detector as long as the latter is able to compute the a posteriori probabilities (APPs) of the data symbols.

This paper is organized as follows: the system model is provided in section II, including a brief description of the turbo detector. In section III we tackle the channel estimation and synchronization problem through the SAGE algorithm, paying special attention to issues related to computational complexity. Numerical results are provided in section IV, before concluding in section V.

II. MC-CDMA UPLINK SYSTEM MODEL

A. Transmitter

We consider the uplink of MC-CDMA system with K_u active users. Each active user transmits frames consisting of M MC symbols to the base station. A frame from the k -th user is generated as follows (see Fig. 1): a block $\mathbf{b}^{(k)} = [b_0^{(k)}, \dots, b_{N_b-1}^{(k)}]^T$ of N_b information-bits is encoded, resulting in N_c coded bits. After interleaving, these N_c coded bits are mapped to a sequence of N_d symbols, belonging to a unit-energy 2^q -point constellation Ω (with $N_d = N_c/q$). After insertion of N_p pilot symbols, we obtain a vector $\mathbf{d}^{(k)} = [d_0^{(k)}, \dots, d_{N_d+N_p-1}^{(k)}]^T$. Now, $\mathbf{d}^{(k)}$ is broken down into M blocks of length P (with $P = (N_d + N_p)/M$). The M blocks are buffered and converted, one at a time, to MC symbols. Let us denote the symbols in the i -th MC symbol of the k -th user as $\mathbf{d}_i^{(k)} = [d_{i,0}^{(k)}, \dots, d_{i,P-1}^{(k)}]^T$. The different notations are explained in Table I.

The conversion of $\mathbf{d}_i^{(k)}$ into a MC-symbol is performed as follows. The p -th data symbol in $\mathbf{d}_i^{(k)}$, $d_{i,p}^{(k)}$, $0 \leq p < P$ is spread by a unit-energy spreading sequence $\mathbf{a}_p^{(k)}$ of length N_s , yielding a sequence of N_s chips $d_{i,p}^{(k)} \times [a_{p,0}^{(k)}, \dots, a_{p,N_s-1}^{(k)}]^T$. Performing spreading for all P symbols in the i -th MC symbol results in a total of $N_s P$ chips. This chip sequence is mapped to $N \doteq N_s P$ subcarriers (known as frequency interleaving). Hence, each of the $N_s P$ chips (say, $d_{i,p}^{(k)} a_{p,s}^{(k)}$) is assigned to a unique subcarrier (say the $n_{p,s}^{(k)}$ -th subcarrier)¹. We end up with a block of N interleaved chips which is provided to an N -point inverse discrete Fourier transform (IDFT), implemented through the fast Fourier transform (FFT) algorithm. A ν -point cyclic prefix (CP) is pre-appended, resulting in $N + \nu$ time-domain samples $[s_{i,-\nu}^{(k)}, \dots, s_{i,-1}^{(k)}, s_{i,0}^{(k)}, \dots, s_{i,N-1}^{(k)}]^T$ where $s_{i,l}^{(k)} = s_{i,l+N}^{(k)}$, for $l = -\nu, \dots, -1$. Hence, the length of the MC symbol is equal to $N_T = N + \nu$. We can write the m -th time-domain sample ($m = -\nu, \dots, N - 1$) of the i -th MC symbol of the k -th user as

$$s_{i,m}^{(k)} = \sqrt{\frac{E_s}{N_T}} \sum_{p=0}^{P-1} \sum_{s=0}^{N_s-1} d_{i,p}^{(k)} a_{p,s}^{(k)} e^{j2\pi n_{p,s}^{(k)} m/N} \quad (1)$$

where E_s denotes the energy per symbol $d_{i,p}^{(k)}$. We further define the MC symbol period T and the sampling period $T_s = T/N_T$. Finally, the signal from the k -th user is shaped with a normalized transmit filter and transmitted over the channel to the base station.

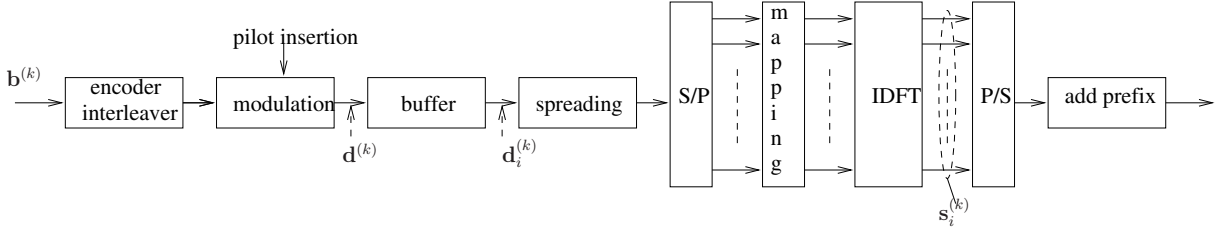
B. Receiver

The base station has to process M MC symbols for each of the K_u users. The signal from the k -th mobile station (the k -th user) to the base station propagates through a channel with overall CIR $h_{\text{ch}}^{(k)}(t - \tau^{(k)})$, where $\tau^{(k)}$ is the propagation delay of the k -th user's signal to the base station. This CIR incorporates the transmit filter, physical propagation channel and receive filter. We assume bursty communication, so that the channel can be modeled as a quasi-static block-fading channel that remains constant during each frame but can vary independently from frame to frame. The code-aided estimation algorithms we will derive can be extended to tracking time-varying channels and synchronization parameters by applying the techniques from [26]. The CIR is assumed to have a delay spread no greater than LT_s for some $L \in \mathbb{N}$, so that $h_{\text{ch}}^{(k)}(t) = 0$ for $t < 0$ and for $t \geq LT_s$. Additionally, the k -th user's signal is affected by a CFO $f_o^{(k)}$. The propagation delay $\tau^{(k)}$ is in some interval³ $[0, \tau_{\text{max}}]$, while the CFO depends on the speed of the mobile station and any possible mismatch between the transmit and receive oscillators. We assume the CFO to be small, compared to the bandwidth of the receiver's matched filter. Hence, the received signal is given by

¹For notational convenience, we will later assume this mapping to be the same for all users. Extension to more general schemes is straightforward.

² L will turn out to be the number of taps of the equivalent discrete-time channel.

³As discussed in [5], the maximum propagation delay τ_{max} can be directly related to the cell radius R : $\tau_{\text{max}} = R/c$, where c is the speed of light. Note that τ_{max} does not depend on the user index k .


 Fig. 1. Frame construction for the k -th user.

$$r(t) = \sum_{k=0}^{K_u-1} s^{(k)}(t) + w(t) \quad (2)$$

where $w(t)$ is the baseband representation of a white Gaussian noise process (with power spectral density $N_0/2$ per real dimension) after suitable filtering. In (2), the signal corresponding to the k -th user contribution can be written as

$$s^{(k)}(t) = \sum_{i=0}^{M-1} \sum_{m=-\nu}^{N-1} s_{i,m}^{(k)} h_{\text{ch}}^{(k)}(t - mT_s - iT_s - \tau^{(k)}) e^{j2\pi f_o^{(k)} t}. \quad (3)$$

The receiver is fully digital and samples the received signal $r(t)$ at a rate $1/T_s$ resulting in a sequence of samples $r(lT_s) = \sum_{k=0}^{K_u-1} s^{(k)}(lT_s) + w(lT_s)$, $l \in \mathbb{Z}$. Let us define the normalized CFO $F^{(k)} = f_o^{(k)} T_s N$. Following [5], we break up $\tau^{(k)}$ as

$$\tau^{(k)} = \Delta^{(k)} T_s - \delta^{(k)} T_s \quad (4)$$

with $\Delta^{(k)} \in \{0, 1, \dots, \Delta_{\max} \doteq \lceil \tau_{\max}/T_s \rceil\}$ and $\delta^{(k)} \in [0, 1]$. Defining $h^{(k)}(t) = h_{\text{ch}}^{(k)}(t + \delta^{(k)} T_s)$, we can express the samples $r(lT_s)$ as a function of $h^{(k)}(t)$. For instance, the contribution to $r(lT_s)$ of the k -th user is given by

$$s^{(k)}(lT_s) = \sum_{i=0}^{M-1} \sum_{m=-\nu}^{N-1} s_{i,m}^{(k)} e^{j2\pi F^{(k)} l/N} \times h^{(k)}(lT_s - mT_s - iN_T T_s - \Delta^{(k)} T_s). \quad (5)$$

Since $T = N_T T_s$ is a multiple of T_s , the channel is fully characterized by the vector

$$\mathbf{h}^{(k)} = [h^{(k)}(0), h^{(k)}(T_s), \dots, h^{(k)}((L-1)T_s)]^T. \quad (6)$$

When $\nu \geq L-1$, no interference between successive MC symbols occurs: for every MC symbol, at least one sequence of N successive time-domain samples exists that does not suffer from interference of the preceding and the following MC symbol⁴. As $\Delta^{(k)} \in \{0, 1, \dots, \Delta_{\max}\}$, samples taken prior to $t = -\nu T_s$ and later than $t = (MT + (\Delta_{\max} + L - \nu - 2)T_s)$ do not depend on the current frame. Hence, the following sequence of time-domain samples is sufficient for synchronization, channel estimation and data detection:

$$\mathbf{r} = [r(-\nu T_s), \dots, r(MT + (\Delta_{\max} + L - \nu - 2)T_s)]^T. \quad (7)$$

The final goal of the base station is to recover the transmit-

⁴When multiple such sequences exist, after conversion to the frequency domain, they lead to equivalent DFT-outputs, up to a known complex rotation (which in no way affects the performance).

ted information bits of the different users \mathbf{b} . As we will see, this requires knowledge of the delay shifts $\Delta^{(k)}$, the (normalized) CFOs $F^{(k)}$ and the CIRs $\mathbf{h}^{(k)}$. Note that information regarding the temporal and frequency misalignment between the users could be sent back to the users so that they can adjust their timing and frequency clocks thereby ensuring that all incoming signals arrive at the base station with the same timing and frequency offsets. Such a synchronous scenario is well understood and leads to very simple receiver design.

C. Turbo detection

Although data detection is not the key contribution of this paper, and the estimation algorithm operates with any detector that is able to compute a posteriori probabilities of the coded symbols, let us, for the sake of clarity, assume we have the following iterative detector. As the users are asynchronous, when detecting the data of any user (say user k) we must remove the multiple access interference (MAI) from other users ($k' \neq k$) in the time domain (TD). This process is known as time-domain multiple access interference cancellation (TD-MAIC). After interference cancellation, we switch to the frequency domain (FD), and perform single user detection. After decoding, the soft information from the decoder is used to reconstruct the TD-signals of the different users and we can again perform TD-MAIC, and so forth. At the first iteration, no TD-MAIC is performed, so we must rely on the spreading to obtain reasonable performance.

Mathematically, this translates to the following. Based on (2) and (II-B) we can re-write the received samples as

$$r(n) = \sum_{k=0}^{K_u-1} \sum_{l=\Delta^{(k)}}^{L+\Delta^{(k)}-1} s_D^{(k)}(n-l) h^{(k)}(l - \Delta^{(k)}) e^{j2\pi F^{(k)} n/N} + w(n) \quad (8)$$

where $w(n)$ is the AWGN contribution, and $s_D^{(k)}(m_i) = s_{i,m}^{(k)}$ with $m_i = iN_T + m$ and $-\nu \leq m \leq N-1$. Assuming we have available soft estimates of the data symbols $\tilde{s}_D^{(k)}(m_i)$ from the FD data detection, these can be used to clean the received signal for detection of user k :

$$r^{(k)}(n) = r(n) - \sum_{k' \neq k, 0}^{K_u-1} \sum_{l=\Delta^{(k')}}^{L+\Delta^{(k')}-1} \tilde{s}_D^{(k')}(n-l) \times h^{(k')}(l - \Delta^{(k)}) e^{j2\pi F^{(k')} n/N}. \quad (9)$$

We then move to the FD by applying the FFT to the cleaned vector at the correct timing and after compensation of the CFO. For user k , MC symbol i , we have the following FFT

output at subcarrier $n_{p,s}$:

$$\begin{aligned} z_{i,p,s}^{(k)} &= \frac{1}{\sqrt{N}} \sum_{l=0}^{N-1} r^{(k)} \left(\Delta^{(k)} + l + iN_T \right) \\ &\quad \times e^{j2\pi l n_{p,s}/N} e^{-j2\pi F^{(k)} (\Delta^{(k)} + l + iN_T)/N} \\ &= d_{i,p}^{(k)} a_{p,s}^{(k)} H_{p,s}^{(k)} \sqrt{\frac{N}{N_T}} E_s + w_{i,p,s} \end{aligned} \quad (10)$$

where $w_{i,p,s}$ contains a thermal noise component as well as the MAI (at the first iteration) or residual uncanceled MAI (at every subsequent iteration). We then apply the multiuser MMSE equalizer from [27] to the vector $\mathbf{z}_{i,p}^{(k)} = [z_{i,p,0}^{(k)}, \dots, z_{i,p,N_s-1}^{(k)}]^T$, resulting in the following equalized samples:

$$\begin{aligned} y_{ip}^{(k)} &= \frac{1}{\sigma_w^2 + \frac{NE_s}{N_T N_s} \sigma_d^2 \sum_{s=0}^{N_s-1} |H_{p,s}^{(k)}|^2} \\ &\quad \left(\sqrt{\frac{NE_s}{N_T}} \sum_{s=0}^{N_s-1} \left(a_{p,s}^{(k)} H_{p,s}^{(k)} \right)^* z_{i,p,s}^{(k)} \right) \end{aligned} \quad (11)$$

Here, for the first iteration we model σ_w^2 as containing thermal noise and the known variance of the MAI. At every subsequent iteration, σ_w^2 consist only of the thermal noise contribution (in other words, residual MAI is ignored). In any case, using a Gaussian approximation, we can determine the so-called extrinsic probabilities $p^{(e)}(d_{i,p}^{(k)}) \propto p(y_{i,p}^{(k)} | d_{i,p}^{(k)})$ which are sent to the demapper and then to the decoder. The decoder computes so-called a priori probabilities $p^{(a)}(d_{i,p}^{(k)})$ regarding the coded symbols (and coded bits), which are combined to obtain soft estimates of the data symbols $\hat{s}_D^{(k)}(m_i)$, used in the next iteration to perform improved TD-MAIC. The detector can also output (approximate) a posteriori probabilities $p(d_{i,p}^{(k)} | \mathbf{r})$ at every iteration, where $p(d_{i,p}^{(k)} | \mathbf{r}) \propto p^{(e)}(d_{i,p}^{(k)}) \times p^{(a)}(d_{i,p}^{(k)})$. The entire receiver operates according to the turbo principle [28], [29].

III. SYNCHRONIZATION AND CHANNEL ESTIMATION

It is clear that the detector described in the previous section requires knowledge regarding the delay shifts⁵ $\Delta^{(k)}$, the CFOs $F^{(k)}$ and the channel taps $\mathbf{h}^{(k)}$. In this section we describe how these parameters can be estimated iteratively. We will first re-write our observation model in a more convenient form in section III-A. In section III-B we will give a brief outline of the SAGE algorithm, and then apply it to our problem in section III-C. Finally, in section III-D we will consider some implementation aspects, and show how the algorithm can be simplified in order to reduce its complexity.

A. Observation Model

We start again from our observation-vector \mathbf{r} from (7). Note that the length of this vector (say, N_{obs}) is independent of $\Delta^{(k)}$.

⁵In correspondence with technical literature, we will name the process of determining Δ *frame synchronization*.

Expanding the observation model in [25], we can express the observation \mathbf{r} as follows

$$\mathbf{r} = \sum_{k=0}^{K_u-1} \mathbf{F}^{(k)} \mathbf{S}_{\Delta^{(k)}}^{(k)} \mathbf{h}^{(k)} + \mathbf{w} \quad (12)$$

where $\mathbf{F}^{(k)}$ is a $N_{\text{obs}} \times N_{\text{obs}}$ diagonal matrix with $\mathbf{F}_{n,n}^{(k)} = e^{j2\pi F^{(k)} n/N}$, $n = -\nu, \dots, N_{\text{obs}} - \nu - 1$ and the vector \mathbf{w} is a zero-mean complex Gaussian random vector with variance $N_0/2$ per real dimension on each of its entries. The $N_{\text{obs}} \times L$ matrix $\mathbf{S}_{\Delta^{(k)}}^{(k)}$ is structured as follows:

$$\mathbf{S}_{\Delta^{(k)}}^{(k)} = \begin{bmatrix} \mathbf{0}_{\Delta^{(k)} \times L} & \\ & \mathbf{S}^{(k)} \\ \mathbf{0}_{(\Delta_{\text{max}} - \Delta^{(k)} + L - 1) \times L} & \end{bmatrix} \quad (13)$$

where $\mathbf{S}^{(k)}$ is a Toeplitz matrix of the pilot and data symbols of the k -th user, and $\mathbf{0}_{L_1 \times L_2}$ is an $L_1 \times L_2$ matrix consisting of all zeros.

MAP estimate: Our goal is to find the maximum a posteriori (MAP) estimate of the delays, CFOs and CIRs of all users. Introducing a vector \mathbf{d}_e containing all these parameters, the MAP estimate is given by

$$\begin{aligned} \hat{\mathbf{d}}_e &= \arg \max_{\mathbf{d}_e} p(\mathbf{d}_e | \mathbf{r}) \\ &= \arg \max_{\mathbf{d}_e} \left\{ p(\mathbf{d}_e) \int p(\mathbf{r} | \mathbf{d}_e, \mathbf{s}) p(\mathbf{s}) d\mathbf{s} \right\} \end{aligned} \quad (14)$$

where \mathbf{s} represents the concatenation of all data symbols of all users. The likelihood-function $p(\mathbf{r} | \mathbf{d}_e, \mathbf{s})$ is given by

$$p(\mathbf{r} | \mathbf{d}_e, \mathbf{s}) \propto \exp \left(-\frac{1}{N_0} \left\| \mathbf{r} - \sum_{k=0}^{K_u-1} \mathbf{F}^{(k)} \mathbf{S}_{\Delta^{(k)}}^{(k)} \mathbf{h}^{(k)} \right\|^2 \right). \quad (16)$$

Finding the MAP estimate is intractable in this case since (a) we need to average over all possible transmitted sequences, and (b), the maximization is over a large-dimensional parameter.

B. The SAGE algorithm

In this section, we will give a brief review of a simplified version the SAGE algorithm [30], which is itself a variation of the expectation-maximization (EM) algorithm [15]. Assume we wish to estimate a parameter \mathbf{d}_e from an observation \mathbf{r} in the presence of a nuisance parameter \mathbf{d}_n . In our case, \mathbf{d}_e corresponds to the CIR, CFO and delays of the K_u users, while \mathbf{d}_n corresponds to the pilot and data symbols of the different users. Finding the MAP estimate of \mathbf{d}_e is usually intractable due to the presence of the nuisance parameters. Furthermore, when \mathbf{d}_e contains many components (as is the case in our problem) finding the MAP estimate requires a multi-dimensional maximization.

The SAGE algorithm avoids these two problems as follows. We break up $\mathbf{d}_e = [\mathbf{d}_{e,1}, \dots, \mathbf{d}_{e,M}]$, where, with a slight abuse of notation, $\mathbf{d}_{e,k} \subseteq \mathbf{d}_e$, and $\mathbf{d}_{e,\bar{k}} \doteq \mathbf{d}_e \setminus \mathbf{d}_{e,k}$. We introduce the *hidden data* $\mathbf{d}_h = [\mathbf{r}, \mathbf{d}_n]$. Given an initial estimate $\hat{\mathbf{d}}_e(0)$ of \mathbf{d}_e , SAGE iterates between an expectation (E) step and a maximization (M) step, for $\xi \geq 1$:

- 1) Select a parameter subset $\mathbf{d}_{e,k}$ to update

2) **E-step**: we update $\mathbf{d}_{e,k}$, while the estimate of $\mathbf{d}_{e,\bar{k}}$ is left unchanged. At iteration ξ , we compute

$$Q\left(\mathbf{d}_{e,k} \mid \hat{\mathbf{d}}_e(\xi-1)\right) = \log p\left(\mathbf{d}_{e,k}, \hat{\mathbf{d}}_{e,\bar{k}}(\xi-1)\right) + \int \log p\left(\mathbf{r} \mid \mathbf{d}_{e,k}, \hat{\mathbf{d}}_{e,\bar{k}}(\xi-1)\right) p\left(\mathbf{d}_n \mid \mathbf{r}, \hat{\mathbf{d}}_e(\xi-1)\right) d\mathbf{d}_n \quad (17)$$

3) **M-step**: update the estimate of $\mathbf{d}_{e,k}$

$$\begin{cases} \hat{\mathbf{d}}_{e,k}(\xi) &= \arg \max_{\mathbf{d}_{e,k}} Q\left(\mathbf{d}_{e,k} \mid \hat{\mathbf{d}}_e(\xi-1)\right) \\ \hat{\mathbf{d}}_{e,\bar{k}}(\xi) &= \hat{\mathbf{d}}_{e,\bar{k}}(\xi-1) \end{cases} \quad (18)$$

Under some mild conditions, the SAGE algorithm guarantees that at every iteration the a posteriori probability of the estimates increases.

C. SAGE estimation for uplink MC-CDMA

We perform estimation under the Bayesian framework and will assume the following a priori distributions of the parameters: the channel taps have a Gaussian distribution with known covariance matrix, so that $p(\mathbf{h}^{(k)}) \propto \exp\left(-(\mathbf{h}^{(k)})^H \Sigma_k^{-1} \mathbf{h}^{(k)}\right)$, while the frequency offsets $F^{(k)}$ and delay $\Delta^{(k)}$ are uniformly distributed over their respective domains. We make the following associations: $\mathbf{d}_{e,k} \leftrightarrow [\Delta^{(k)}, F^{(k)}, \mathbf{h}^{(k)}]$ and $\mathbf{d}_n \leftrightarrow \mathbf{s}$. We will denote the estimates at the ξ -th iteration of the SAGE algorithm as $\hat{\Delta}^{(k)}(\xi)$, $\hat{F}^{(k)}(\xi)$ (and $\hat{\mathbf{F}}^{(k)}(\xi)$), and $\hat{\mathbf{h}}^{(k)}(\xi)$. We start from an initial estimate of $\mathbf{d}_{e,k}$, for all $k = 0, \dots, K_u - 1$, provided through a conventional DA algorithm. The SAGE algorithm then becomes, at the ξ -th iteration (see Fig. 2):

- 1) Select a user for which to update the delay, CFO and CIR estimate. Say we select user k
- 2) **E-step**: now (17) becomes, after some straightforward manipulations (see [31])

$$Q\left(\mathbf{d}_{e,k} \mid \hat{\mathbf{d}}_e(\xi-1)\right) \simeq \frac{2}{N_0} \Re\left(\left(\mathbf{h}^{(k)}\right)^H \left(\mathbf{F}^{(k)} \tilde{\mathbf{S}}_{\Delta^{(k)}}^{(k)}\right)^H \tilde{\mathbf{x}}^{(k)}\right) - \frac{1}{N_0} \left(\mathbf{h}^{(k)}\right)^H \left(\tilde{\mathbf{C}}_{\Delta^{(k)}}^{(k)} + N_0 \Sigma_k^{-1}\right) \mathbf{h}^{(k)} \quad (19)$$

where

$$\tilde{\mathbf{x}}^{(k)} = \mathbf{r} - \sum_{k'=0, k' \neq k}^{K_u-1} \hat{\mathbf{F}}^{(k')}(\xi-1) \tilde{\mathbf{S}}_{\Delta^{(k')}(\xi-1)}^{(k')} \hat{\mathbf{h}}^{(k')}(\xi-1) \quad (20)$$

while

$$\tilde{\mathbf{S}}_{\Delta^{(k)}}^{(k)} = \int \mathbf{S}_{\Delta^{(k)}}^{(k)} p\left(\mathbf{s} \mid \mathbf{r}, \hat{\mathbf{d}}_e(\xi-1)\right) d\mathbf{s} \quad (21)$$

and

$$\tilde{\mathbf{C}}_{\Delta^{(k)}}^{(k)} = \int \left(\mathbf{S}_{\Delta^{(k)}}^{(k)}\right)^H \mathbf{S}_{\Delta^{(k)}}^{(k)} p\left(\mathbf{s} \mid \mathbf{r}, \hat{\mathbf{d}}_e(\xi-1)\right) d\mathbf{s}. \quad (22)$$

We will show how the matrices $\tilde{\mathbf{S}}_{\Delta^{(k)}}^{(k)}$ and $\tilde{\mathbf{C}}_{\Delta^{(k)}}^{(k)}$ can be computed in the next section.

3) **M-step**: now we update the estimates of $\Delta^{(k)}$ and $F^{(k)}$:

$$\begin{aligned} & \left[\hat{\Delta}^{(k)}(\xi), \hat{F}^{(k)}(\xi)\right] = \\ & \arg \max_{\Delta^{(k)}, F^{(k)}} \left\{Q\left(\mathbf{d}_{e,k} \mid \hat{\mathbf{d}}_e(\xi-1)\right)\right\} \end{aligned} \quad (23)$$

where the maximization can be solved by any appropriate numerical technique. Note that the 2-dimensional maximization in (23) can be reduced to two 1-dimensional maximizations when the CFO is small [5] [25]. For the CIR, a closed-form solution is given by

$$\hat{\mathbf{h}}^{(k)}(\xi) = \left(\tilde{\mathbf{C}}_{\hat{\Delta}^{(k)}}^{(k)} + N_0 \Sigma_k^{-1}\right)^{-1} \tilde{\mathbf{S}}_{\hat{\Delta}^{(k)}(\xi)}^H \left(\hat{\mathbf{F}}^{(k)}(\xi)\right)^H \tilde{\mathbf{x}}^{(k)}. \quad (24)$$

We see that the SAGE estimator requires the knowledge of the channel covariance matrix Σ_k and the noise power N_0 . These can reasonably be assumed to be known at the receiver, since these quantities change only very slowly over time, compared to the duration of a burst.

D. Practical considerations

Computation of $\tilde{\mathbf{S}}_{\Delta^{(k)}}^{(k)}$ and $\tilde{\mathbf{C}}_{\Delta^{(k)}}^{(k)}$: The matrix $\tilde{\mathbf{S}}_{\Delta^{(k)}}^{(k)} = \int \mathbf{S}_{\Delta^{(k)}}^{(k)} p\left(\mathbf{s} \mid \mathbf{r}, \hat{\mathbf{d}}_e(\xi-1)\right) d\mathbf{s}$ is obtained by replacing each entry $s_{i,m}^{(k)}$ in $\mathbf{S}_{\Delta^{(k)}}^{(k)}$ with the corresponding a posteriori expectation

$$\begin{aligned} \tilde{s}_{i,m}^{(k)} &= \int s_{i,m}^{(k)} p\left(\mathbf{s} \mid \mathbf{r}, \hat{\mathbf{d}}_e(\xi-1)\right) d\mathbf{s} \\ &= \sqrt{\frac{E_s}{N_T}} \sum_{p=0}^{P-1} \sum_{s=0}^{N_s-1} \mathbb{E}\left[d_{i,p}^{(k)} \mid \mathbf{r}, \hat{\mathbf{d}}_e(\xi-1)\right] \\ &\quad \times a_{p,s}^{(k)} e^{j2\pi n_{p,s} m / N}. \end{aligned} \quad (25)$$

We know from section II-C that the detector computes the a posteriori probabilities (APPs) of the coded symbols $p\left(d_{i,p}^{(k)} \mid \mathbf{r}, \hat{\mathbf{d}}_e(\xi-1)\right)$, so that

$$\mathbb{E}\left[d_{i,p}^{(k)} \mid \mathbf{r}, \hat{\mathbf{d}}_e(\xi-1)\right] = \sum_{\omega \in \Omega} \omega \times p\left(d_{i,p}^{(k)} = \omega \mid \mathbf{r}, \hat{\mathbf{d}}_e(\xi-1)\right) \quad (27)$$

which can be interpreted as a soft symbol decision: it is a weighted average of all possible constellation points. Note that for pilot symbols, $\mathbb{E}\left[d_{i,p}^{(k)} \mid \mathbf{r}, \hat{\mathbf{d}}_e(\xi-1)\right]$ is simply equal to the known pilot symbol $d_{i,p}^{(k)}$.

The matrix $\tilde{\mathbf{C}}_{\Delta^{(k)}}^{(k)}$ cannot be computed exactly based on the a posteriori probabilities of the coded symbols but, thanks to the presence of the interleaver, we can approximate $\tilde{\mathbf{C}}_{\Delta^{(k)}}^{(k)}$ as

$$\tilde{\mathbf{C}}_{\Delta^{(k)}}^{(k)} \approx \left(\tilde{\mathbf{S}}_{\Delta^{(k)}}^{(k)}\right)^H \tilde{\mathbf{S}}_{\Delta^{(k)}}^{(k)}. \quad (28)$$

When the symbol sequence is sufficiently long, $\tilde{\mathbf{C}}_{\Delta^{(k)}}^{(k)}$ can be approximated by a diagonal matrix.

Initialization: The SAGE algorithm can be initialized with any known data-aided or blind channel estimation/synchronization algorithm. A most elegant way to initialize is by using the SAGE algorithm in data-aided mode. This means that we set the entries in $\tilde{\mathbf{S}}_{\Delta^{(k)}}^{(k)}$ and $\tilde{\mathbf{C}}_{\Delta^{(k)}}^{(k)}$ that

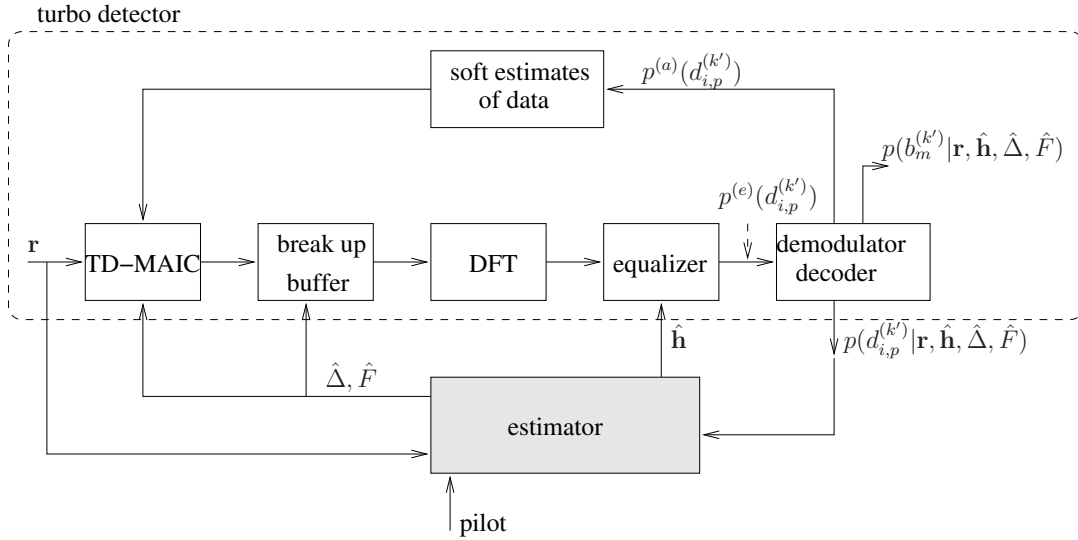


Fig. 2. Detector and estimator for the k' -th user. The box in grey is the focus of this paper.

correspond to the coded symbols to zero (since we have no a priori information from the detector); the entries that correspond to the pilot symbols are of course set to their (known) values. We then proceed as follows. Since the CFO is assumed to be small, we initialize $\hat{F}^{(k)}(0)$ to 0, $\forall k$. Since this implies that $\hat{\mathbf{F}}^{(k)}(0) = \mathbf{I}$, we can easily determine $\hat{\Delta}^{(k)}(0)$ and $\hat{\mathbf{h}}^{(k)}(0)$ (see also [25], section III.B).

Complexity: To reduce the complexity of the SAGE estimator, we can introduce the following approximations:

- In principle, every time we update a parameter estimate $\hat{\mathbf{d}}_{e,k}$, we need to re-compute the APPs $p(d_{i,p}^{(k)} | \mathbf{r}, \hat{\mathbf{d}}_e)$. This requires resetting the turbo detector and performing many turbo detection iterations. To avoid this overhead, we prefer to perform *embedded estimation* [32]: when a parameter $\hat{\mathbf{d}}_{e,k}$ is updated, the turbo detector is not reset, but maintains state information (in the form of the extrinsic and a priori probabilities) from the previous turbo detector iteration. In that case, the overhead related to SAGE estimation becomes reasonable.
- Conversely, for fixed APPs $p(d_{i,p}^{(k)} | \mathbf{r}, \hat{\mathbf{d}}_e)$, we can update multiple parameters estimates $\hat{\mathbf{d}}_{e,k}$. For instance, we could update the parameters $\hat{\mathbf{d}}_{e,k}$ for *all* users (rather than just a single user), while keeping the APPs fixed.
- In case the delay $\Delta^{(k)}$ and the CFO $F^{(k)}$ are perfectly known (or when their estimates have converged), the SAGE algorithm of the channel impulse response can take place completely in the frequency domain, thus avoiding FFT operations at each SAGE update. This requires a specific frequency-domain observation model [26]. This is not pursued in the current paper.

The resulting computational complexity can be quantified as follows. When we denote by T_D the time (in seconds) to perform a single iteration in the turbo detector, and by T_{Sage} the time to update the parameters of all the users for given APPs, then the overhead related to embedded SAGE

estimation is given by (see [25]):

$$O_{\text{est}} = \frac{I_{\text{sage}}}{I_{\text{sage}} + 1} \times \frac{T_{\text{sage}}}{T_D} \quad (29)$$

where I_{sage} is the number of iterations between the detector and the SAGE estimator. The values of T_D and T_{sage} depend on the specific implementation of the detector and the SAGE estimator. As is detailed in [25], the complexity tends to be dominated by the updating of the delay estimates, and is of the order $\mathcal{O}(K_u N_T (N_d + N_p) L \Delta_{\text{max}})$.

IV. NUMERICAL RESULTS

In this section we will compare the performance of the data-aided (DA) and the code-aided (CA) estimation algorithms.

A. Simulation Parameters

To validate the proposed algorithms, we have carried out Monte Carlo simulations. We considered a system with $K_u = 5$ users, using a $R = 1/3$ rate turbo-code consisting of two constituent systematic recursive rate one-half convolutional codes with generators $(21, 37)_8$. A block length of $N_b = 368$ information bits was chosen, leading to $N_c = 1104$ coded bits. Coded bits are Gray-mapped onto an 8-PSK constellation resulting in $N_d = 368$ data symbols to which $N_p = 16$ pilots 8-PSK symbols are appended for initial channel parameter estimation. This sequence of $N_d + N_p = 384$ 8-PSK symbols is broken up into $M = 12$ blocks of $P = 32$ 8-PSK symbols per block. Spreading sequences are real-valued Walsh-Hadamard sequences, with chips belonging to $\left\{ -\frac{1}{\sqrt{N_s}}, +\frac{1}{\sqrt{N_s}} \right\}$ and have a length $N_s = 16$, leading to $N = PN_s = 512$ required subcarriers. The channel has length $L = 15$ and is modeled with independent components, each being a zero-mean complex Gaussian random variable with an exponential power delay profile:

$$\mathbb{E} \left[\left(h^{(k)}(l) \right)^* h^{(k')}(l') \right] = \delta_{k-k'} \delta_{l-l'} \sigma_{h^{(k)}}^2 \exp(-l/5), \quad l = 0, \dots, L-1 \quad (30)$$

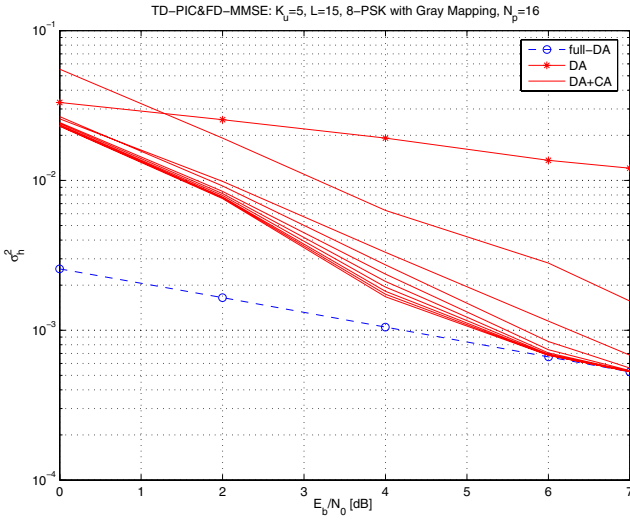


Fig. 3. channel estimation: variance of the estimated CIRs for synchronous users for different iterations (from top to bottom).

where $\sigma_{\hat{h}^{(k)}}^2$ is chosen such that the average energy per subcarrier is normalized to unity. Hence, the energy of the channel is concentrated mainly in the first few channel taps. This model leads to a diagonal matrix Σ_k , so that the matrix inversion in (24) when updating $\hat{\mathbf{h}}^{(k)}$ (ξ) is trivial, under the assumption that $\tilde{\mathbf{C}}_{\Delta^{(k)}}^{(k)}$ can be well-approximated by a diagonal matrix. To avoid ISI, a cyclic prefix of length $\nu = 14$ is employed. The reference propagation delay and CFO are $\Delta = 17$ and $F = 0$ respectively. The timing shifts $\Delta^{(k)}$ are fixed to 7, 11, 25, 37, 17 for $k = 1, \dots, 5$, respectively. We will assume a small CFO, so that the 2-dimensional maximization in (23) can be reduced to two 1-dimensional line-searches. Performance will be evaluated in terms of mean squared estimation error (MSEE) and bit-error-rate (BER). Where applicable, the BER will be compared to a system with full knowledge of the channel and synchronization parameters, while the MSEE will be compared to an estimator which has perfect knowledge of all data symbols (referred to as the full-DA estimator).

B. Channel estimation for synchronous transmission

We first investigate the estimation of the CIRs $\mathbf{h}^{(k)}$, assuming synchronous users⁶, i.e. $F^{(k)} = 0$ and $\Delta^{(k)} = 17$ for $k = 0, \dots, K_u - 1$. In figures 3 and 4 we compare the performance of the MSEE of the channel taps and the corresponding BER obtained with the increasing number of SAGE iterations ξ . We observe a significant improvement resulting from iterating between detector and channel estimator. Furthermore, for $E_b/N_0 \geq 6$ dB the CA estimator is able to achieve the lower bound of the full-DA estimator.

C. Joint synchronization and channel estimation for asynchronous transmission

We consider frame synchronization, jointly with channel and CFO estimation. As the MSEEs of the timings $\Delta^{(k)}$ do not

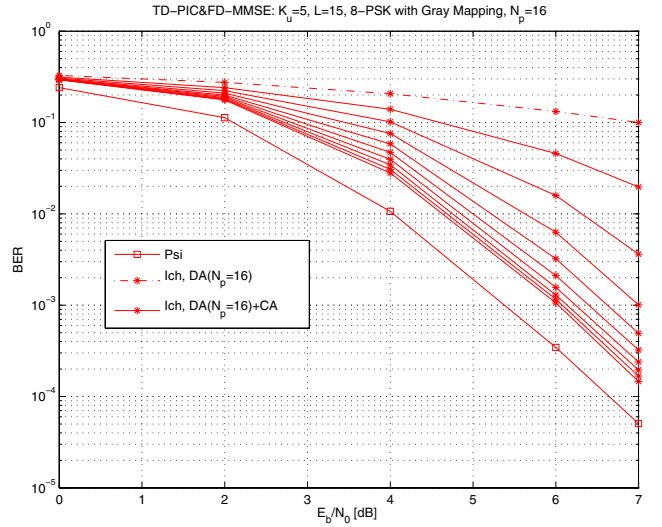


Fig. 4. channel estimation: BER for 5 synchronous users, Psi stands for perfect knowledge of synchronization and CIR, Ich stands for Imperfect CIR knowledge.

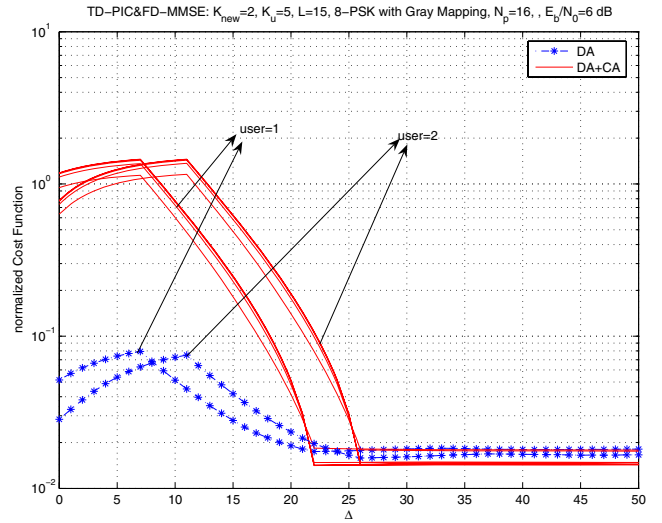


Fig. 5. Joint frame-frequency synchronization and channel estimation: trial value of Δ vs. MAP timing cost function at 6 dB for two new users accessing the system ($K_{\text{new}} = 2$) using $\hat{F}^{(k)}(\xi = 0) = 0$ as a frequency initial estimate. $F^{(k)}$ is selected randomly such that $|F^{(k)}| < 0.007$, $k = 0, \dots, K_{\text{new}} - 1$. The true frame shifts are $\Delta^{(0)} = 7$ and $\Delta^{(1)} = 11$.

give a clear picture, in Figure 5 we take a look at the average cost function $Q(\mathbf{d}_{e,k} | \hat{\mathbf{d}}_e(\xi - 1))$ for the timing delays $\Delta^{(k)}$ of two new users accessing the system (denoted by $K_{\text{new}} = 2$), at $E_b/N_0 = 6$ dB. For both data-aided estimation and SAGE estimation, the cost functions are maximized at $\Delta^{(0)} = 7$ and $\Delta^{(1)} = 11$, which corresponds to the actual values of $\Delta^{(0)}$ and $\Delta^{(1)}$ respectively. Fig. 6 depicts the average probability mass function⁷ (pmf) of ϵ_{Δ} after estimation. Note that even at $E_b/N_0 = 6$ dB, the SAGE-based frame synchronizer will produce timing errors lying in the ISI free region almost 100% of the time. Fortunately, the situation where $\epsilon_{\Delta} < 0$ is not very critical. In fact, if $L - \nu - 1 \leq \epsilon_{\Delta} < 0$, the

⁷Note that this pmf is actually defined as the average of two pmfs relative to the two new users accessing the system.

⁶Note in this case the SAGE can be implemented completely in the FD.

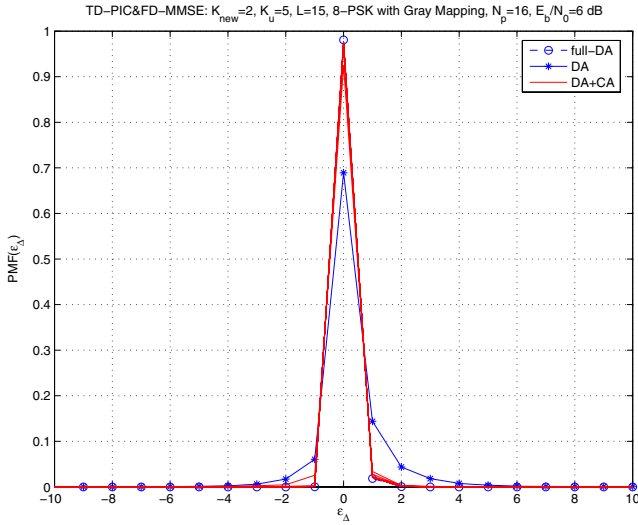


Fig. 6. Joint frame-frequency synchronization and channel estimation: pmf of timing estimation error at $E_b/N_0 = 6$ dB for two new users accessing the system ($K_{\text{new}} = 2$) using $\hat{F}^{(k)}(\xi = 0) = 0$ as a frequency initial estimate. $F^{(k)}$ is selected randomly such that $|F^{(k)}| < 0.007$, $k = 0, \dots, K_{\text{new}} - 1$. The true frame shifts are $\Delta^{(0)} = 7$ and $\Delta^{(1)} = 11$.

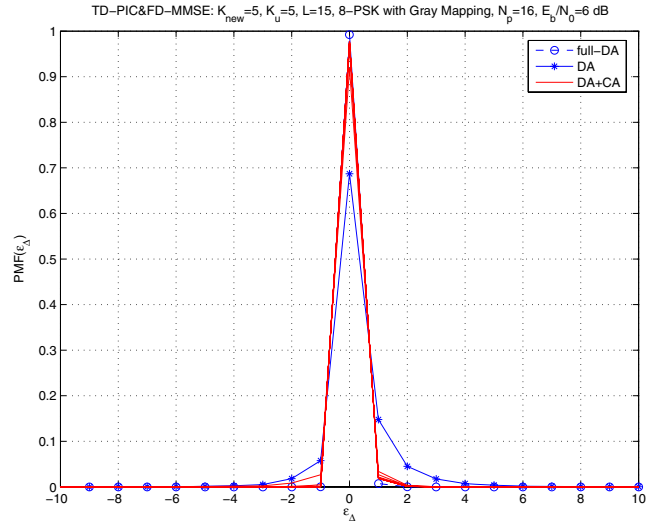


Fig. 8. Joint frame-frequency synchronization and channel estimation: pmf of timing estimation error at $E_b/N_0 = 6$ dB for 5 new users accessing the system ($K_{\text{new}} = 5$) using $\hat{F}^{(k)}(\xi = 0) = 0$ as a frequency initial estimate. $F^{(k)}$ is selected randomly such that $|F^{(k)}| < 0.007$, $k = 0, \dots, K_u - 1$.

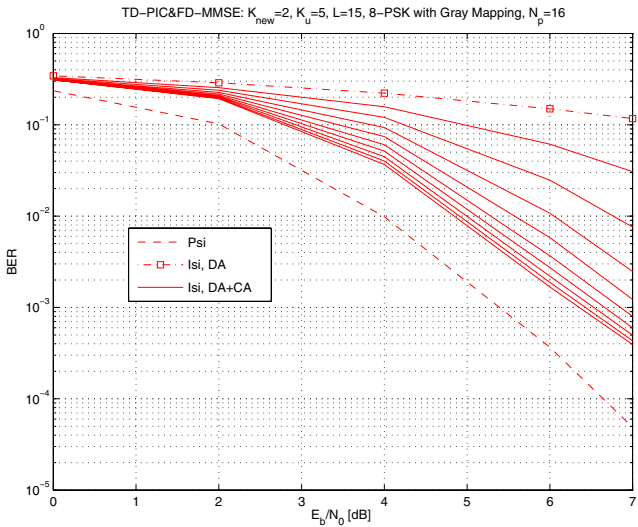


Fig. 7. Joint frame-frequency synchronization and channel estimation: BER performance for two new users accessing the system ($K_{\text{new}} = 2$) using $\hat{F}^{(k)}(\xi = 0) = 0$ as a frequency initial estimate. $F^{(k)}$ is selected randomly such that $|F^{(k)}| < 0.007$ for $k = 0, \dots, K_{\text{new}} - 1$. The true frame shifts are $\Delta^{(0)} = 7$ and $\Delta^{(1)} = 11$. Psi stands for perfect knowledge of synchronization and CIR, Isi stands for joint synchronization and channel estimation.

frame synchronization error will not destroy the orthogonality among the subcarriers [5]. On the other hand, when $\epsilon_{\Delta} > 0$, the estimate of \mathbf{h} will not capture the dominant components, which can have a severe impact on the detection performance. From Fig. 6, we see that the latter situation occurs rarely with the data-aided and SAGE-based estimators. Moreover, it can be noticed that the CA estimator yields a pmf close to the full-DA estimator. The improvement by embedding estimation in the detection, can be further confirmed when showing the BER resulting from the joint MAP estimation of all parameters, in Fig. 7. As expected, the DA estimator gives rise to large degradations, whereas the SAGE based estimator yields a close

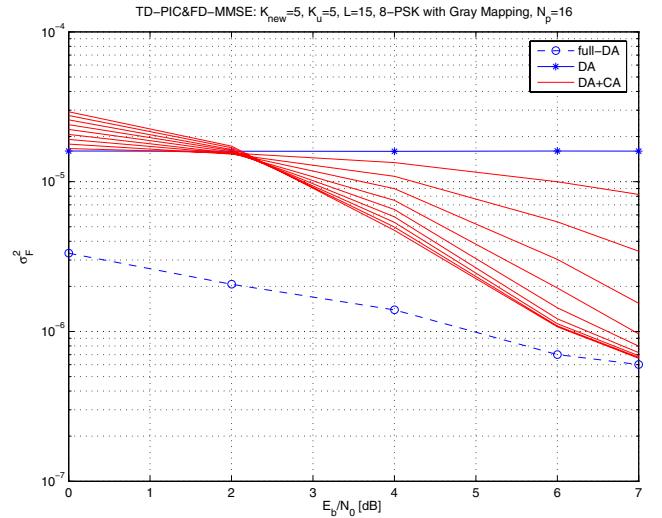


Fig. 9. Joint frame-frequency synchronization and channel estimation: MSEE of CFO estimation error for 5 new users accessing the system ($K_{\text{new}} = 5$) using $\hat{F}^{(k)}(\xi = 0) = 0$ as a frequency initial estimate. $F^{(k)}$ is selected randomly such that $|F^{(k)}| < 0.007$, $k = 0, \dots, K_u - 1$.

to optimal performance (less than 1 dB performance loss).

Figures 8, 9 and 10 report the pmf of the timing, the MSEE of the estimated CFO and the BER respectively when all 5 active users are asynchronous. Again, impressive performance gain results by exploiting the available APPs from the iterative detector in the SAGE-based estimator and only 1 dB performance loss occurs with respect to optimal BER. For $E_b/N_0 \geq 6$ dB, the CA MSEE of the CFO is close to the MSEE of the full-DA estimator.

V. CONCLUSIONS

We have investigated an asynchronous MC-CDMA uplink receiver with bit-interleaved coded modulation, performing joint iterative multi-user data detection, synchronization and channel estimation. To remove the need for long training

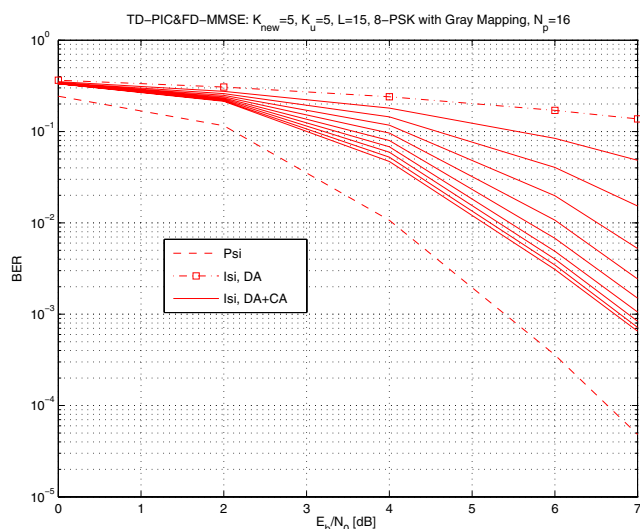


Fig. 10. Joint frame-frequency synchronization and channel estimation: BER performance for 5 users accessing the system ($K_{\text{new}} = 5$) using $\hat{F}^{(k)}(\xi = 0) = 0$ as a frequency initial estimate. $F^{(k)}$ is selected randomly such that $|F^{(k)}| < 0.007$, $k = 0, \dots, K_u - 1$. Psi stands for perfect knowledge of synchronization and CIR, Isi stands for joint synchronization and channel estimation.

sequences, we have considered the SAGE algorithm as a tool to perform iterative estimation. It turns out that the SAGE estimator is most suited for the particular estimation problems we have considered. The estimator operates by accepting soft information from the detector, in the form of a posteriori probabilities (APPs) of the coded symbols. Furthermore, the computational overhead related to estimation was minimized by introducing simple modifications to the SAGE-based estimator.

The performance of the proposed code-aided estimation algorithm was evaluated in terms of BER and MSEE through Monte Carlo simulations. We demonstrated that the SAGE-based algorithm, exploiting information from all data symbols, significantly outperforms the conventional corresponding data-aided algorithms.

REFERENCES

- [1] J. A. C. Bingham, "Multicarrier modulation: an idea whose time has come," *IEEE Commun. Mag.*, vol. 28, no. 5, pp. 5–14, May 1990.
- [2] S. Nanda, R. Walton, J. Ketchum, M. Wallace, and S. Howard, "A high-performance MIMO OFDM wireless LAN," *IEEE Commun. Mag.*, vol. 43, no. 1, pp. 53–60, Jan. 2005.
- [3] T. Pollet, M. Van Bladel, and M. Moeneclaey, "BER sensitivity of OFDM systems to carrier frequency offset and Wiener phase noise," *IEEE Trans. Commun.*, vol. 43, no. 2-3-4, pp. 191–193, Feb.-Mar.-Apr. 1995.
- [4] H. Steendam and M. Moeneclaey, "Synchronization sensitivity of multicarrier systems," *European Trans. Commun.*, ETT special issue on multicarrier spread spectrum, vol. 52, no. 5, pp. 834–844, May 2004.
- [5] M. Morelli, "Timing and frequency synchronization for the uplink of an OFDMA system," *IEEE Trans. Commun.*, vol. 52, pp. pp.296–306, Feb. 2004.
- [6] T. M. Schmidl and D. C. Cox, "Robust frequency and timing synchronization for OFDM," *IEEE Trans. Commun.*, vol. 45, pp. pp.1613–1621, Dec. 1997.
- [7] M. Morelli and U. Mengali, "A comparison of pilot-aided channel estimation methods for OFDM systems," *IEEE Trans. Signal Processing*, vol. 49, no. 12, pp. 3065–3073, Dec. 2001.
- [8] M. Speth, S. A. Fechtel, G. Fock, and H. Meyr, "Optimum receiver design for wireless broad-band systems using OFDM, part I," *IEEE Trans. Commun.*, vol. 47, no. 11, pp. 1668–1677, Nov. 1999.
- [9] M. Speth, S. Fechtel, G. Fock, and H. Meyr, "Optimum receiver design for OFDM-based broadband transmission, part II: a case study," *IEEE Trans. Commun.*, vol. 49, no. 4, pp. 571–579, Apr. 2001.
- [10] E. G. Larsson, G. Liu, J. Li, and G. B. Giannakis, "Joint symbol timing and channel estimation for OFDM based WLANs," *IEEE Commun. Lett.*, vol. 5, no. 8, pp. 325–327, Aug. 2001.
- [11] Y. Yao and G. B. Giannakis, "Blind carrier frequency offset estimation in SISO, MIMO, and multiuser OFDM Systems," *IEEE Trans. Commun.*, vol. 53, no. 1, Jan. 2005.
- [12] M. Tanda, "Blind symbol-timing and frequency offset estimation in OFDM systems with real data symbols," *IEEE Trans. Commun.*, vol. 52, no. 10, pp. 1609–1612, Oct. 2004.
- [13] M. C. Necker and G. L. Stuber, "Totally blind channel estimation for OFDM on fast varying mobile radio channels," *IEEE Trans. Wireless Commun.*, vol. 3, no. 5, pp. 1514–1525, Sept. 2004.
- [14] C. Berrou, A. Glavieux, and P. Thitimajshima, "Near Shannon limit error-correcting coding and decoding: turbo codes," in *Proc. IEEE ICC'94*, pp. 1064–1070.
- [15] A. P. Dempster, N. M. Laird, and D. B. Rubin, "Maximum likelihood from incomplete data via the EM algorithm," *J. Royal Statistical Society*, vol. 39, no. 1, pp. 1–38, 1977, series B.
- [16] N. Noels, V. Lottici, A. Dejonghe, H. Steendam, M. Moeneclaey, M. Luise, and L. Vandendorpe, "A Theoretical framework for soft information based synchronization in iterative (turbo) receivers," *EURASIP J. Wireless Commun. and Networking (JWCN)*, special issue on advanced signal processing algorithms for wireless communications, vol. 2005, no. 2, pp. 117–129, Apr. 2005.
- [17] G. A. Al-Rawi, T. Y. Al-Naffouri, A. Bahai, and J. Cioffi, "Exploiting error-control coding and cyclic prefix in channel estimation for coded OFDM systems," *IEEE Commun. Lett.*, vol. 7, no. 7, pp. 388–390, July 2003.
- [18] C. H. Aldana, E. de Carvalho, and J. M. Cioffi, "Channel estimation for multicarrier multiple input single output systems using the EM algorithm," *IEEE Trans. Signal Processing*, vol. 51, no. 12, pp. 3280–3292, Dec. 2003.
- [19] T. Y. Al-Naffouri, O. Awoniyi, O. Oteri, and A. Paulraj, "Receiver design for MIMO-OFDM transmission over time variant channels," in *Proc. IEEE Globecom*, Dallas, TX, Dec. 2004.
- [20] S. Y. Park, Y. G. Kim, and C. G. Kang, "Iterative receiver for joint detection and channel estimation in OFDM systems under mobile radio channels," *IEEE Trans. Veh. Technol.*, vol. 53, no. 2, pp. 450–460, Mar. 2004.
- [21] J. J. Beek, P. O. Borjesson, M. Boucheret, D. Landstom, J. Arenas, P. Odling, C. Ostberg, M. Whalqvist, and S. Wilson, "A time and frequency synchronization scheme for multiuser OFDM," *IEEE J. Select. Areas Commun.*, vol. 17, no. 11, pp. pp. 1900–1914, 1999.
- [22] M. O. Pun, M. Morelli, and C. J. Kuo, "Maximum likelihood synchronization and channel estimation for OFDMA uplink transmissions," *IEEE Trans. Commun.*, vol. 54, no. 4, pp. pp. 726–736, 2006.
- [23] —, "Iterative detection and frequency synchronization for generalized OFDMA uplink transmissions," *IEEE Trans. Wireless Commun.*, Dec. 2006.
- [24] L. Sanguinetti and M. Morelli, "Channel acquisition and tracking for MC-CDMA uplink transmissions," *IEEE Trans. Veh. Technol.*, vol. 55, no. 3, pp. 956–967, May 2006.
- [25] M. Guenach, H. Wymeersch, H. Steendam, and M. Moeneclaey, "Code-aided ML joint frame synchronization and channel estimation for downlink MC-CDMA," *IEEE J. Select. Areas Commun.*, vol. 24, no. 6, pp. 1105–1114, June 2006.
- [26] H. Wymeersch, F. Simoons, and M. Moeneclaey, "Code-aided channel tracking for OFDM," in *Proc. IEEE International Symposium on Turbo Codes & Related Topics*, Munich, Apr. 2006.
- [27] X. Wang and H. V. Poor, "Iterative (turbo) soft interference cancellation and decoding for coded CDMA," *IEEE Trans. Commun.*, vol. 47, no. 7, pp. pp.1046–1061, July 1999.
- [28] S. ten Brink, J. Speidel, and J. C. Yan, "Iterative demapping and decoding for multilevel modulation," in *Proc. IEEE GLOBECOM'98*, 1998.
- [29] F. Kschischang, B. Frey, and H.-A. Loeliger, "Factor graphs and the sum-product algorithm," *IEEE Trans. Inform. Theory*, vol. 47, no. 2, pp. pp.498–519, Feb. 2001.
- [30] J. A. Fessler and A. O. Hero, "Space-alternating generalized expectation-maximization algorithm," *IEEE Trans. Signal Processing*, vol. 42, no. 10, pp. 2664–2677, Oct. 1994.
- [31] H. Wymeersch, "Software radio algorithms for coded transmission," Ph.D. dissertation, Ghent University, Ghent, Belgium, 2005.

- [32] V. Lottici and M. Luise, "Embedding carrier phase recovery into iterative decoding of turbo-coded linear modulations," *IEEE Trans. Commun.*, vol. 52, no. 4, pp. 661–669, Apr. 2004.



Mamoun Guenach (S'99, M'03) is currently a research engineer with Alcatel-Lucent Bell Labs, Antwerp, Belgium. In 1995, he received the degree of engineer in electronics and communications from the Ecole Mohamadia d'Ingenieurs in Morocco. Following that, he moved to the faculty of applied sciences at the Universite Catholique de Louvain (UCL), Louvain-La-Neuve, Belgium, where he received a M.S. degree in electricity and a Ph.D. degree in applied sciences in 1997 and 2002 respectively. Between 2002 and 2006, he served as a post-

doctoral researcher in the department of telecommunications and information processing at the University of Gent, Belgium before he joined Alcatel-Lucent Bell Labs Antwerp, Belgium.



Mohamed Marey received the B.Sc. and M.Sc. degree in electrical engineering from Menoufia University, Menouf, Egypt, in 1995 and 1999 respectively. He worked as an instructor and assistant lecturer in the department of Communication Engineering, Menoufia university in 1996-1999 and 1999-2004 respectively. In 2004, he was granted a fund for scientific research from the government of the Arab Republic of Egypt to prepare Ph.D., towards which he is currently working within the Department of Telecommunications and Information

Processing, Ghent University, Belgium. His main research interests include synchronization, channel estimation, coding, and interference cancellation for wireless multi-carrier communication systems. He is the author of several scientific papers. He received the young scientist award from International Union of Radio Science (URSI) in 1999.



Henk Wymeersch Henk Wymeersch received the diploma of computer science engineer and Ph.D. degree in applied sciences at Ghent University, Belgium, in 2001 and 2005, respectively. Between 2001 and 2005 he was with the Department of Telecommunications and Information Processing at Ghent University. Currently, he is a postdoctoral fellow of the Belgian-American Educational Foundation and is affiliated with the Laboratory for Information and Decision Systems at the Massachusetts Institute of Technology (MIT). His research interests include channel coding, synchronization, iterative processing and sensor networks.



Heidi Steendam received the M.Sc. degree in Electrical Engineering and the Ph.D. degree in Applied Sciences from Ghent University, Ghent, Belgium in 1995 and 2000, respectively. Since September 1995, she has been with the Digital Communications (DIGCOM) Research Group, Department of Telecommunications and Information Processing (TELIN), Faculty of Engineering, Ghent University, Belgium, first in the framework of various research projects, and since October 2002 as a full time Professor in the area of Digital Communications.

Her main research interests are in statistical communication theory, carrier and symbol synchronization, bandwidth-efficient modulation and coding, spread-spectrum (multi-carrier spread-spectrum), satellite and mobile communication. She is the author of more than 80 scientific papers in international journals and conference proceedings.

Since 2002, she is an executive Committee Member of the IEEE Communications and Vehicular Technology Society Joint Chapter, Benelux Section. She has been active in various international conferences as Technical Program Committee member and Session chair. In 2004, she was the conference chair of the IEEE Symposium on Communications and Vehicular Technology in the Benelux.

She is teaching courses on Data Communications, Information Theory and Advanced Modulation and Coding Techniques.

Marc Moeneclaey received the Diploma and the Ph.D. Degree, both in electrical engineering, from Ghent University, Ghent, Belgium, in 1978 and 1983, respectively. He is currently a Professor in the Department of Telecommunications and Information Processing at Ghent University. His main research interest are in statistical communication theory, carrier and symbol synchronization, bandwidth-efficient modulation and coding, spread spectrum, satellite and mobile communication. He is the author of about 300 scientific papers in international journals and conference proceedings. Together with H. Meyr (RWTH Aachen) and S. Fechtel (Siemens AG), he is coauthor of the book *Digital Communication Receivers - Synchronization, Channel Estimation, and Signal Processing* (New York: Wiley, 1998)